Original Article

miR-328-3p overexpression attenuates the malignant proliferation and invasion of liver cancer via targeting Endoplasmic Reticulum Metallo Protease 1 to inhibit AKT phosphorylation

Hua Lu[1#], Jiali Hu[2#], Jianping Li[3], Weifeng Lu[1], Xiaofan Deng[4], Xu Wang[5]

[1]Anesthesia Operation Center, [2]Department of Pain, [3]Department of Geriatrics, [4]Organ Transplant Center, [5]Department of Hepatobiliary Surgery, Sichuan Academy of Medical Sciences & Sichuan Provincial People's Hospital, Chengdu, China

Contributions: (I) Conception and design: J Li, W Lu; (II) Administrative support: H Lu, J Hu; (III) Provision of study materials or patients: J Li, W Lu; (IV) Collection and assembly of data: H Lu, J Hu; (V) Data analysis and interpretation: H Lu, J Hu; (VI) Manuscript writing: All authors; (VII) Final approval of manuscript: All authors.

[#]These authors contributed equally to this work.

Correspondence to: Jianping Li. Department of Geriatrics, Sichuan Academy of Medical Sciences & Sichuan Provincial People's Hospital, Chengdu, China. Email: kehui04224244@163.com; Weifeng Lu. Anesthesia Operation Center, Sichuan Academy of Medical Sciences & Sichuan Provincial People's Hospital, Chengdu, China. Email: vowof096849@sina.cn.

Background: Liver cancer is one of the most common cancers worldwide. microRNAs (miRNAs) have been recognized as minimally invasive prognostic markers for distinct types of cancer. This study evaluates the mitigation role of miR-328-3p on liver cancer *in vitro* and *in vivo*.

Methods: Liver cancer cell line Huh-7 and HepG2 were used for *in vitro* experiments. Compared with the control group, miR-328-3p overexpression inhibited the proliferation, invasion, and promoted apoptosis of Huh-7 cells. miR-328-3p and endoplasmic reticulum metalloprotease 1 (*ERMP1*) had an excellent targeting relationship. Compared with the pcDNA-*ERMP1* transfection group, the ratios of p-PI3K/PI3K, p-AKT/AKT, and p-mTOR/mTOR in miR-328-3p mimic and pcDNA-*ERMP1* co-transfection group were significantly decreased. Animal models were set up using four-week-old immunodeficient BABL/c female nude mice. Huh-7 cells transfected with lentivirus holding miR-328-3p or empty vector were injected into the right dorsal side of BABL/c nude mice, respectively. Tumor volume was measured every five days. After one month, animals were sacrificed, xenograft tumors were dissected and weighed for RT-PCR and immunohistochemical assays.

Results: Compared with control group, miR-328-3p overexpression significantly inhibited tumor weight (0.46±0.07 *vs.* 0.11±0.05 g, P<0.05) and tumor volume (1876±321 *vs.* 543±168 mm^3, P<0.05) after thirty days. miR-328-3p overexpression significantly downregulated the percentage of Ki67 positive cells, N-cadherin positive cells and vimentin positive cells.

Conclusions: These findings suggested that miR-328-3p could be a new treatment or a novel marker for liver cancer prognosis.

Keywords: Liver cancer; invasion; miR-328-3p; Huh-7 cells; apoptosis

Submitted Apr 10, 2020. Accepted for publication Jun 11, 2020.
doi: 10.21037/atm-20-3749
View this article at: http://dx.doi.org/10.21037/atm-20-3749

Introduction

Liver cancer is a malignant liver tumor, which can be divided into two categories: primary and secondary. Primary liver malignancies originate from the epithelial or mesenchymal tissue of the liver. The former is called primary liver cancer, which is a high incidence in China and is extremely harmful. The latter is called sarcoma and is less common than primary liver cancer. Secondary or metastatic liver cancer refers to the invasion of the liver by malignant tumors originating from multiple organs throughout the body (1,2). Treatment methods usually include surgery, chemotherapy, and radiation therapy. Biological therapy, traditional Chinese medicine, and traditional Chinese medicine for liver cancer are also widely used; however, because its mechanisms are not apparent, targeted treatment cannot be performed. Hence, it is necessary to find new therapeutic strategies and drugs.

microRNAs (miRNAs) are endogenous, noncoding RNAs, with approximately 22 nucleotides that regulate gene expression by combining with the 3'untranslated region (3'UTR) of miRNAs to suppress translation or induction of miRNAs cleavage (3). miRNAs have been recognized to be important in the regulation of cancer and have been proposed as minimally invasive prognostic markers for various types of cancer (4-6). To date, multiple miRNAs have taken part in liver cancer regulation. Zhang *et al.* reported that miR-34a could negatively regulate the expression of lactate dehydrogenase A (*LDHA*), which consequently inhibited *LDHA*-dependent glucose uptake in the cancer cells (5). Simultaneously, miR-34a could inhibit cell proliferation and invasion of cancer cells. The results showed that miR-34a functions as a negative regulator of glucose metabolism and might be a novel marker for liver cancer prognosis. Li *et al.* reported that mirRNA-210 silence exerted inhibition effect in the progression of liver cancer and hepatitis B virus-associated liver cancer via targeting *EGR3* (7).

Cancer stem cells (CSCs) in liver cancer are recognized to handle tumor recurrence and metastasis. However, the factors that mediate this mechanism have yet to be completely elucidated. PI3K (phosphatidylinositol 3-kinase)/AKT (also known as protein kinase B) pathway plays a vital role in CSCs, including the ability to maintain colony-formation ability and proliferation (8). At the same time, targeting the PI3K/AKT pathway could remarkably reduce the bulk tumor burden and slow down CSCs metabolism (9,10). Sun *et al.* reported that FAK (Focal adhesion kinase)/PI3K/Akt and p38 MAPK signaling pathways could promote the migration of dental pulp stem cells (11). miR-328-3p is used for the regulation of many cancers (12-15), and PI3K/Akt signaling pathway is one of its participating pathways (16,17). Pan *et al.* found that miR-328-3p exerted inhibition of cell proliferation and metastasis effect in colorectal cancer by targeting Girdin and inhibiting the PI3K/Akt signaling pathway (17).

Endoplasmic Reticulum Metallo Protease 1 (*ERMP1*) is a novel potential oncogene involved in oxidative stress defense, and unfolded protein response (*UPR*) is highly expressed in human cancer. Endoplasmic reticulum (ER) stress is highly activated in cancer and involved in tumorigenesis and resistance to anti-cancer therapy. Researchers reported that *ERMP1* is involved in the development of multiple cancers, such as ovary cancers, colorectal, breast, and childhood acute myeloid leukemia (18,19). They found that inhibition of *ERMP1* expression significantly suppressed proliferation, migration, and invasiveness of cancer cells. Qu *et al.* investigated the tumor-suppressive role of miR-148b targeted *ERMP1* in endometrial cancer cells. They found that *ERMP1* was a good target of miR-148b, and miR-148b could suppress cell proliferation and regulated the oxidative stress response by downregulating *ERMP1* (20).

Although miR-328-3p participated in the regulation of cancer processes, whether miR-328-3p exerted the inhibitory effect via the PI3K/AKT pathway targeting *ERMP1* was unknown. In the present study, the Huh-7 cell line was selected as the experimental cell line and explored the anti-tumor effect of miR-328-3p overexpression on liver cancer. The results showed that overexpressed miR-328-3p inhibited cell proliferation, invasion, and induced apoptosis. TargetScan software predicts that miR-328-3p can directly bind to the 3'-UTR region of the *ERMP1* gene. Notably, compared with *ERMP1* transfection alone, the co-transfection of miR-328-3p with *ERMP1* reduced the colony formation rate and weakened the phosphorylation of PI3K/AKT. The results of the *in vivo* tumor transplantation model were consistent with the results of *in vitro* experiments. The results showed that miR-328-3p overexpression inhibited PI3K/AKT pathway to attenuate the malignant proliferation and invasion of liver cancer via targeting *ERMP1*. These findings suggested that overexpressed miR-328-3p could be a new adjuvant against liver cancer.

We present the following article in accordance with the ARRIVE reporting checklist (available at http://dx.doi.

org/10.21037/atm-20-3749).

Methods

Cell culture

The liver cancer cell lines Huh-7 cells (https://web.expasy.org/cellosaurus/ CVCL_0336) and HepG2 cells (https://web.expasy.org/cellosaurus/CVCL_0027) were purchased from American Type Culture Collection (ATCC, Manassas, VA). Cells were cultured in RPMI 1640 Medium (Invitrogen, Carlsbad, CA) with 10% FBS, 100 U/mL penicillin, and 100 U/mL streptomycin under standard culture conditions, 2–3 passages. Treatment was all done in basal medium supplemented with 5% heat-inactivated fetal bovine serum.

Cell transfection

ERMP1 cDNA and miR-328-3p mimics were synthesized by Molbase biological reagent company. After PCR amplification, *ERMP1* cDNA was inserted into the pcDNA3.1 plasmid. Huh-7 cells and HepG2 cells were seeded in 6-well plates. After reaching 70–80% confluence, the cells were transfected with Lipofectamine 2000 transfection reagents (Invitrogen, Carlsbad, CA, USA). Upon transfection for 6 h, fresh medium was replaced. Cells were harvested at 48 h after transfection. Transfection efficiency was confirmed using RT-PCR and Western blot. Cells were performed in five groups: Control group, mimic-NC group, miR-328-3p mimic group, pcDNA-*ERMP1* group, and miR-328-3p mimic + pcDNA-*ERMP1* (mimic + *ERMP1*) group. Epithelial-mesenchymal transition (EMT) of each group cells were observed by optical microscope (Leica, Germany).

Colony formation assay

5×10^3 Huh-7 cells were seeded in triplicate to 6-well plates overnight for colony formation assays. After ten days of culture, visible cells were washed with phosphate-buffered saline (PBS), fixed with methanol, and then stained with Giemsa. Colonies with N50 cells were counted.

Transwell assay

The matrigel was diluted with serum-free medium and then applied to the middle bottom of the upper chamber. Air-dry at room temperature for later use. The cell suspension was added into the upper chambers (200 mL per chamber) incubating for 24 hours with serum-free medium. The lower chambers were filled with 600 μL medium holding 10% FBS. As incubation at 37 ℃ for 24 h, the chambers were removed and washed twice with PBS. The residual cells were cleared by cotton bud. After fixed with 95% alcohol and stained with crystal violet, cells were examined by a microscope (Leica, Germany), and the average amount of invasive cells was recorded. The experiments were independently repeated in triplicate.

Flow cytometry

Upon transfected with miR-328-3p mimic and pcDNA-*ERMP1*, the cell apoptosis rate in sphere-forming cells was measured, referring to the testing instructions. Briefly, the detection of cell apoptosis rate was performed with the manufacturer's protocol and measured by flow cytometry analysis.

Real-time polymerase chain reaction (RT-PCR)

Total RNA from cells and tissues was extracted using a TRIzolTM kit following the manufacturer's protocol. After quantification, 0.5 μg RNA of each sample was used to synthesize cDNA with a cDNA Synthesis kit. miR-328-3p mimic and the *ERMP1* expression level was determined by the SYBRPCR MasterMix kit with GAPDH as an internal reference to normalize individual gene expression according to the $2^{-\Delta\Delta Ct}$ method (21). The primers used in the experiments were all designed using the Primer3Plus website and synthesized by Suzhou Jinweizhi Biotechnology Co., Ltd. The experiment was repeated three times.

The primers sequence as following:

miR-328-3p forward primer: 5'-CGGGCCTGGCCC TCTCTGCC-3'; miR-328-3p reverse primer: 5'-CAGCC ACAAAAGAGCACAAT-3';

ERMP1 forward primer: 5'-ACGCGGCTGTCTCTTT TC-3'; *ERMP1* reverse primer : 5'-CTTGGCACCAGTG CCATTAT-3'.

Actin forward primer: 5'-AGGTCATCACTATTGGCA AC-3'; Actin reverse primer :5'-ACTCATCGTACTCCT GCTTG.

Luciferase reporter assay

TargetScan software revealed that *ERMP1* is one of miR-328-3p's targets. The wild-type (WT) fragments from

ERMP1 (*ERMP1*-WT) containing the potential binding sites and corresponding mutant type (MUT) fragments (*ERMP1*-MUT) of miR-328-3p were inserted into the pMIR-report plasmid vector (Promega, USA) to generate the *ERMP1* luciferase reporter construct. Then, the vectors and miR-328-3p mimics were co-transfected into Huh-7 cells using Lipofectamine 2000 reagent (Invitrogen, Carlsbad, CA, USA) (22). Twenty-four hours after transfection, the cells were assayed using a luciferase detection kit (Promega, 09 Madison, WI, United States). Recording the ratio of Rluc/Luc.

Tumor formation assay

Animal models were set up using four-week-old immunodeficient BABL/c female nude mice. All mice were kept free of specific pathogens. For tumor formation assays, Huh-7 cells transfected with lentivirus holding miR-328-3p or empty vector were injected subcutaneously into BABL/c nude mice, respectively. Tumor volume was measured every 5 days. Thirty days after injection, animals were sacrificed, xenograft tumors were dissected and weighed for RT-PCR and immunohistochemical assays.

The animal experiments in present study were carried out according to the Guidelines for the Care and Use of NIH Experimental Animals and approved by Sichuan Academy of Medical Sciences & Sichuan Provincial People's Hospital.

Immunohistochemistry (IHC)

IHC assay was performed as previously described (23). Paraffin sections were separated in xylene and rehydrated in gradient ethanol. After the antigen was extracted in 10 mM citric acid buffer, the tissue sections were incubated in 3% H_2O_2 for 10 min and sealed at room temperature for 1 h. The tissue sections were then incubated overnight with Ki67, N-cadherin, vimentin, miR-328-3p and *ERMP1* (CST, Danvers, MA, USA), respectively. Sections were then washed with TBST and incubated with SignalStain® Boost IHC Detection Reagent for 30 min at room temperature. After that, sections were stained with a SignalStain DAB Substrate Kit and observed under an optical microscope. All experiments were in triplicate.

Immunohistofluorescence-confocal microscopy

The immunofluorescent assay was manipulated to estimate the level of AKT in Huh-7 cells, which affect by miR-328-3p overexpression. Huh-7 cells were seeded onto small glass dishes and transfected with miR-328-3p. Liver cancer Huh-7 cells infected by the lentivirus were visualized by immunofluorescence in 14 μm frozen sections using an anti-EGFP polyclonal antibody (Molecular Probes, Eugene, OR; 1:800, overnight incubation at 4 ℃). Cell nuclei were stained with Hoescht. The experiment procedure was according to previously reported (24).

TUNEL assay

The prepared paraffin sections were dewaxed, rehydrated, and washed. The detection is based on the principle of *in situ* DNA nicked-end labeling technique. Briefly, cell apoptosis were detected using an FD Apop Kit (FD NeuroTechnologies, Ellicott City, MD) according to manufacturer's instructions. Apoptosis cells were detected by fluorescence microscopy (Olympus, Japan).

Western blot analysis

Western blot was determined by reference (25). The primary antibodies were as follow: Ki-67 (ab15580, 1:500), PCNA (ab92552, 1:1,000), E-cadherin (ab1416, 1:50), N-cadherin (ab18203, 1:300), caspase-3 (ab13847, 1:500), cleaved caspase-3 (ab2302, 1:500), poly ADP-ribose polymerase (PARP) (ab74290, 1:1,000), Bax (ab32503, 1:1,000), Bcl-2 (ab196495, 1:500), PI3K (ab140307, 1:2,000), p-PI3K (ab154598, 1:1,000), AKT (ab8805, 1:500), p-AKT (ab38449, 1:1,000), mTOR (ab2732, 1:2,000), p-mTOR (ab109268, 1:1,000). The internal reference for western blot analysis is β-Actin (ab179467, 1:5,000). The relative protein level was analyzed by ImageJ software. The experiments were independently repeated in triplicate.

Statistical analysis

The statistical analysis was conducted with SPSS 21.0 (SPSS, Inc., Chicago, IL, USA). Data were presented as the mean ± SD. Multiple sets of data were analyzed by one-way ANOVA, followed by Bonferroni post-hoc test. Differences were considered statistically significant when $P<0.05$.

Results

miR-328-3p targets ERMP1

As shown in *Figure 1A*, miR-328-3p was underexpressed

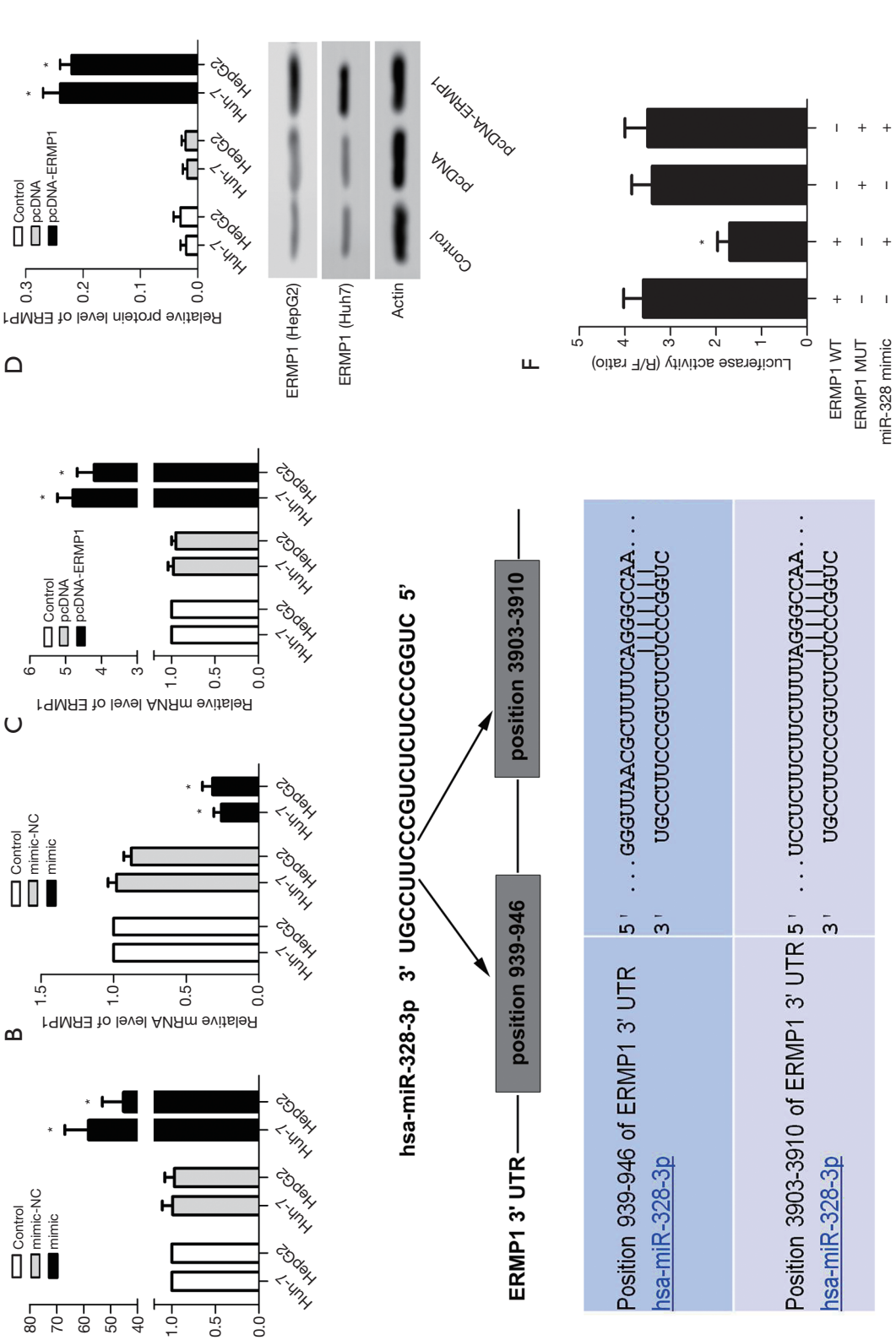

Figure 1 miR-328-3p targets *ERMP1*. (A) The relative level of miR-328-3p in Huh-7 and HepG2 cells transfected with miR-328-3p mimic; (B) relative mRNA level of *ERMP1* in Huh-7 and HepG2 cells transfected with miR-328-3p mimic; (C) relative mRNA level of *ERMP1* in Huh-7 and HepG2 cells transfected with pcDNA-*ERMP1*; (D) the relative protein level of *ERMP1* in Huh-7 and HepG2 cells transfected with pcDNA-*ERMP1*; (E) targetScan search software predicts that miR-328-3p can directly bind to the 3'-UTR region of the *ERMP1* gene; (F) Luciferase activity (R/F ratio). *, P<0.05 *vs.* control.

in liver cancer cells Huh-7 and HepG2. Compared with the control group, miR-328-3p expression was increased significantly in the miR-328-3p mimic transfected group. This showed that miR-328-3p successfully transfected liver cancer cells Huh-7 and HepG2, which means that stable liver cancer cell lines were set up. Compared with the control group, the relative mRNA level of *ERMP1* in Huh-7 and HepG2 cells were decreased after transfected with miR-328-3p mimic (*Figure 1B*). As expected, relative mRNA and protein levels of *ERMP1* were increased by pcDNA-*ERMP1* transfected (*Figure 1C,D*). Notably, there are hardly differences between HepG2 cells and Huh7 cells with the expression of miR-328-3p and *ERMP1*. Huh7 cells were used in subsequent studies. TargetScan search software predicts that miR-328-3p can directly bind to the 3'-UTR region of the *ERMP1* gene (*Figure 1E*).

Double luciferase reporter assay showed that miR-328-3p could significantly inhibit the fluorescence intensity of *ERMP1* 3'-UTR-WT vector ($P<0.05$), but could not inhibit the fluorescence intensity of *ERMP1* 3'-UTR-MUT vector (*Figure 1F*). The result suggested that miR-328-3p and *ERMP1* had a good targeting relationship.

miR-328-3p overexpression counteracts ERMP1 induction of Huh-7 cell growth

Compared with the control group, miR-328-3p overexpression in the miR-328-3p mimic transfected group significantly inhibited colony formation rate in Huh-7 cells (*Figure 2A*). As shown in *Figure 2B*, miR-328-3p overexpression significantly elevated the cell apoptosis rate of Huh-7 cells. As shown in *Figure 2C*, miR-328-3p overexpression significantly reduced the expression of Ki67 in Huh-7 cells, with a significant increase of cleaved cas3/cas3 and Bax/Bcl-2. These results show that overexpressed miR-328-3p has the effects of reducing colony formation rate, inhibiting proliferation, and promoting apoptosis in Huh-7 cells.

miR-328-3p overexpression inhibits the athletic ability of Huh-7 cells

As shown in *Figure 3A*, compared with the control group, miR-328-3p overexpression significantly reduced the number of invasive cells per field, while *ERMP1* overexpression significantly enhanced the number of invasive cells per field in Huh-7 cells. Compared with the *ERMP1* group, the mimic + *ERMP1* group significantly reduced the number of invasive cells per field. The result suggested that overexpression of miR-328-3p inhibits the invasion of Huh-7 cells (*Figure 3A*). EMT is an important part of the process of tumor deterioration. During the progress of EMT, cells lose their epithelial traits, including cell adhesion and polarity, and obtain a mesenchymal morphology and the ability to migrate. miR-328-3p overexpression significantly mitigated the EMT of Huh-7 cells (*Figure 3B*). Significantly, miR-328-3p overexpression increased the expression of E-cadherin in Huh-7 cells accompanied by a significant decrease of N-cadherin expression (*Figure 3C*). These results show that overexpressed miR-328-3p suppresses the invasion of Huh-7 cells.

miR-328-3p overexpression inhibits AKT phosphorylation

Western blot assay was performed to detect the activation of PI3K/AKT in liver cancer cells. As shown in *Figure 4A*, miR-328-3p mimic transfection inhibited the phosphorylation of PI3K, AKT, and mTOR in liver cancer cells. Compared with the pcDNA-*ERMP1* transfection group, the ratios of p-PI3K/PI3K, p-AKT/AKT, and p-mTOR/mTOR in miR-328-3p mimic and pcDNA-*ERMP1* co-transfection group were significantly decreased (*Figure 4A*). The immunofluorescent assay was manipulated to estimate the level of AKT in Huh-7 cells, which affect by miR-328-3p overexpression. Compared with the control group, miR-328-3p overexpression significantly reduced AKT^+ puncta per nucleus, while *ERMP1* overexpression significantly enhanced AKT^+ puncta per nucleus in Huh-7 cells. Compared with the *ERMP1* group, the mimic + *ERMP1* group significantly reduced AKT^+ puncta per nucleus (*Figure 4B*). These results show that miR-328-3p inhibits AKT phosphorylation by targeting *ERMP1*.

miR-328-3p overexpression affects tumor formation in vivo

A transplanted tumor model was set up by subcutaneously injecting Huh-7 cells with stable miR-328-3p expression into female nude mice to verify the effect of miR-328-3p on tumor formation *in vivo*. Smaller volume and lighter weight of transplanted tumors were observed in a miR-328-3p group compared with the control group (*Figure 5A,B,C*). Compared with the control group, miR-328-3p overexpression significantly downregulated the level of *ERMP1* (*Figure 5D*). Immunohistochemical results showed that the percentage of Ki67 positive cells, N-cadherin

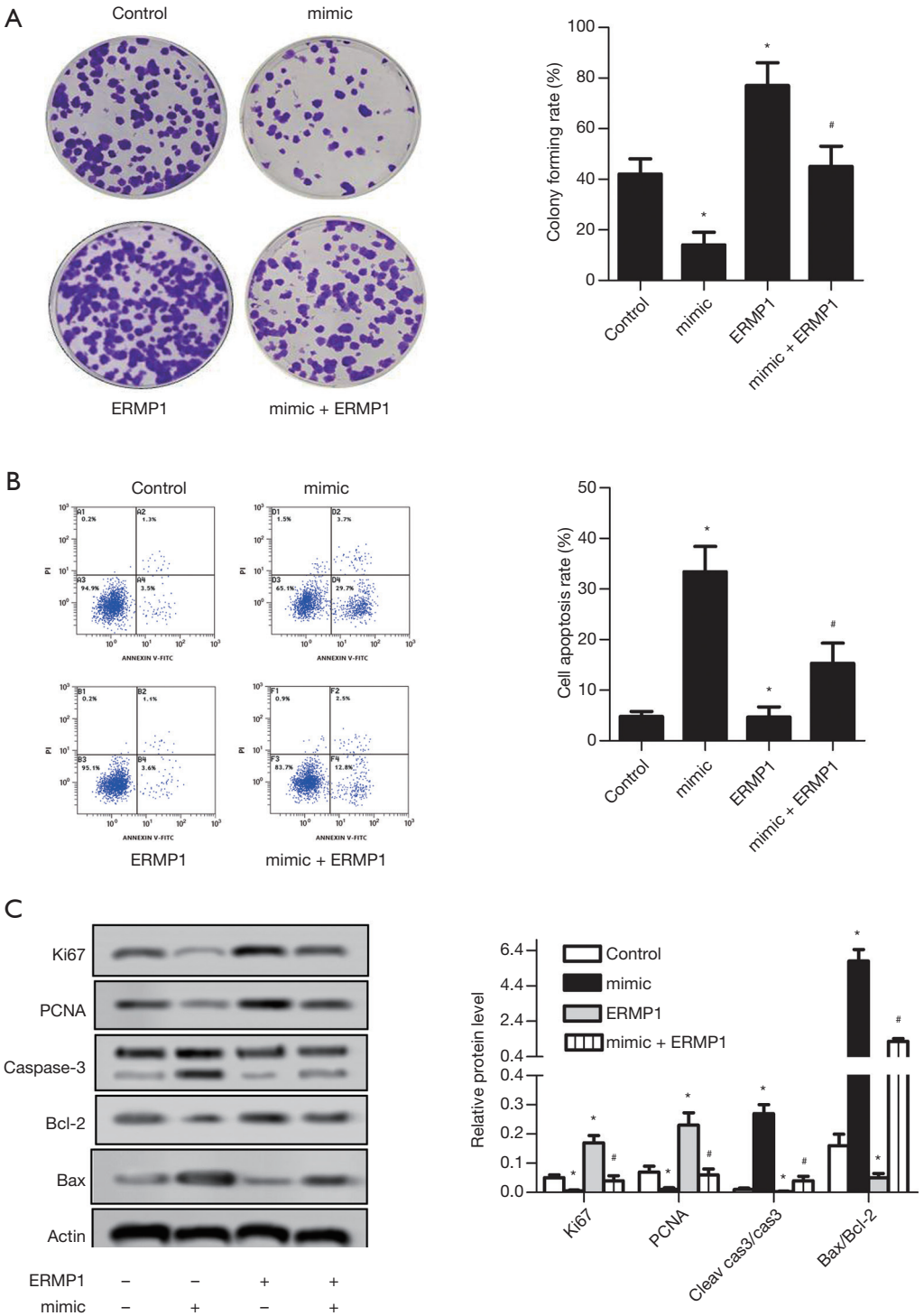

Figure 2 miR-328-3p overexpression counteracts *ERMP1* induction of Huh-7 cell growth. (A) The typical image of colony formation assay (stained with Giemsa, ×400 magnification) and percentage of colony formation rate; (B) the typical image of flow cytometry and the percentage of colony formation rate cell apoptosis rate; (C) miR-328-3p overexpression inhibited the proliferation of Huh-7 cells. Data are expressed as mean ± SD of three independent experiments. *, P<0.05 *vs.* control; #, P<0.05 *vs. ERMP1* group.

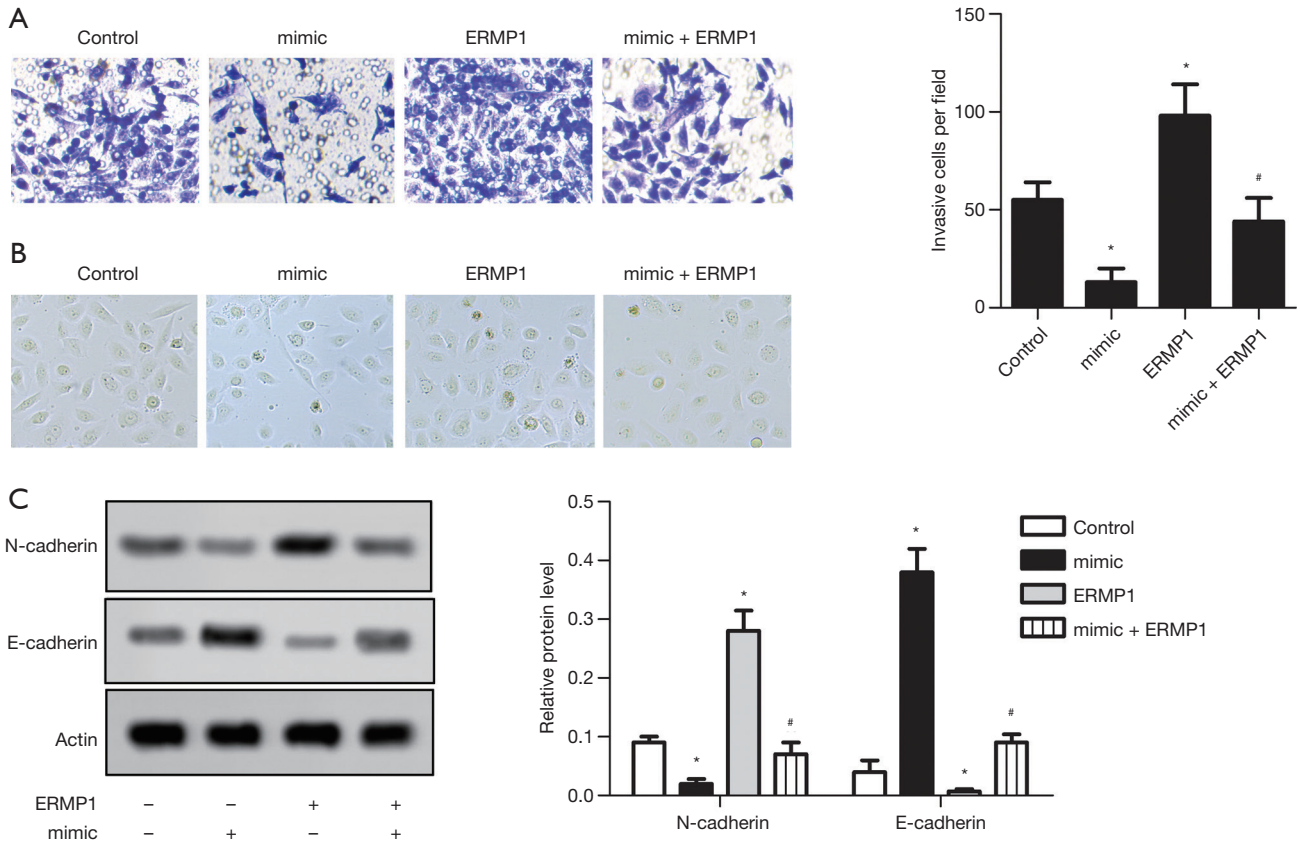

Figure 3 miR-328-3p overexpression inhibits the athletic ability of Huh-7 cells. (A) The typical image of transwell assay (stained with crystal violet, ×400 magnification) and invasive cells per field; (B) miR-328-3p overexpression inhibits EMT of Huh-7 cells (×400 magnification); (C) miR-328-3p overexpression increased the expression of E-cadherin and decreased the expression of N-cadherin in Huh-7 cells. Data are expressed as mean ± SD of three independent experiments. *, P<0.05 *vs.* control; #, P<0.05 *vs. ERMP1* group.

positive cells and vimentin positive cells in the miR-328-3p group were significantly lower than the control group (*Figure 5D*). Western blot assay was used to detect relative protein level of caspase-3, cleaved caspase-3 and PARP to analyze apoptosis. From *Figure 5E*, the ratio of cleav cas3/cas3 and the expresion of PARP were enhanced significantly in miR-328-3p group. Western blot assay also used to assess the phosphorylation level of AKT. As shown in *Figure 5F*, compared with the control group, miR-328-3p overexpression significantly reduced the ratio of p-AKT/AKT. These results show that overexpression of miR-328-3p inhibits tumor formation *in vivo*.

Discussion

Liver cancer is a malignant liver tumor, which can be divided into two categories: primary and secondary. Primary liver malignancies originate from the epithelial or mesenchymal tissue of the liver, which is a high incidence in China and is seriously harmful. Biological therapies have been considered for the treatment of liver cancer (26). Because its mechanism is unclear, it has become the top priority of medical research. miRNAs have been widely used in the diagnosis and treatment of liver cancer (27,28). In our study, overexpressed miR-328-3p inhibited cell proliferation, invasion, and induced apoptosis of liver cancer cell line Huh-7. Consistent with the results of *in vitro* experiments, miR-328-3p overexpression significantly inhibited tumor growth and volume increase *in vivo* experiments. These results revealed that miR-328-3p could be a novel gene therapy for liver cancer.

The regulation of miR-328-3p has been locked as a potential therapeutic strategy for a variety of cancers. Xiao *et al.* found that overexpression of miR-328-3p and miR-

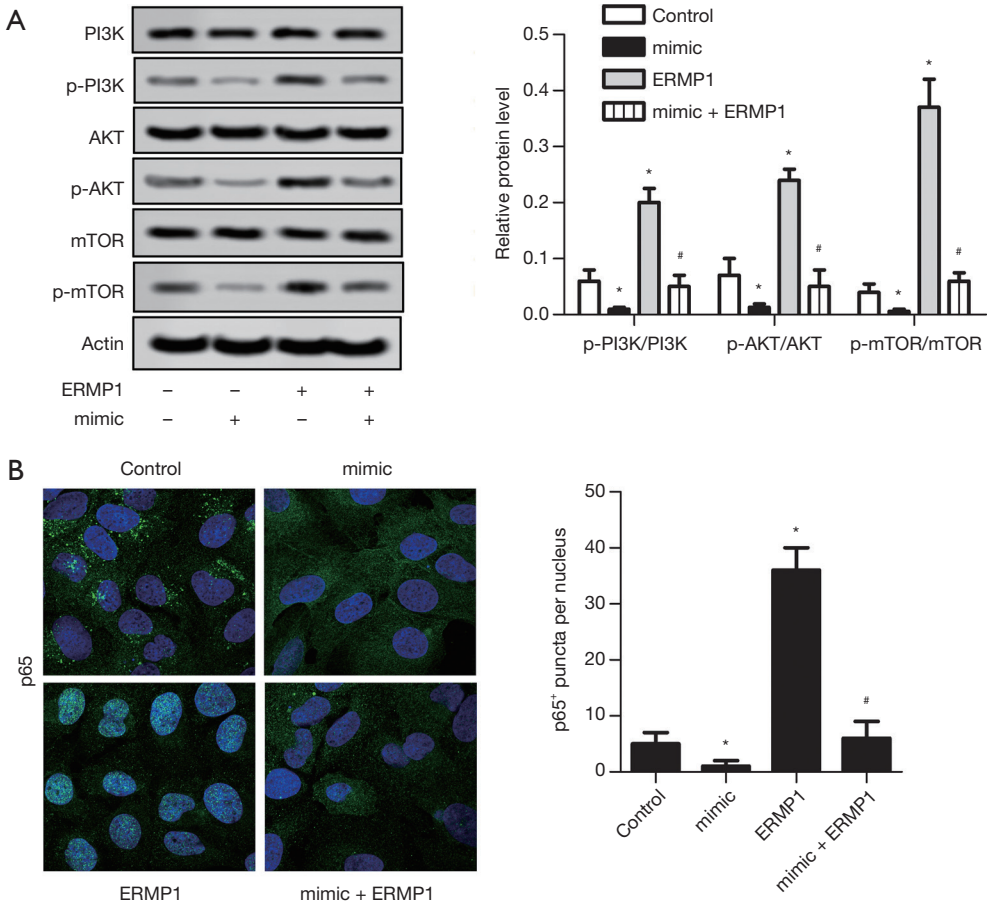

Figure 4 miR-328-3p overexpression inhibits AKT phosphorylation. (A) The typical image of western blot assay and the ratio of p-PI3K/PI3K, p-AKT/AKT, and p-mTOR/mTOR; (B) typical immunofluorescence image and AKT^{+} puncta per nucleus (stained with Hoescht, ×400 magnification). Data are expressed as mean ± SD of three independent experiments. *, P<0.05 *vs.* control; $^{\#}$, P<0.05 *vs. ERMP1* group.

370-3p counteracted the inhibitory effect of GRM4-induced cell proliferation, invasion, and migration (15). Ma *et al.* reported that miR-328-3p upregulation sensitizes non-small cell lung cancer to radiotherapy (14). These results were consistent with our findings. In our study, miR-328-3p was lowly expressed in Liver cancer cell line Huh-7. Compared with the control group, miR-328-3p overexpression in the miR-328-3p mimic transfected group significantly inhibited colony formation rate and reduced the expression of Ki67 in Liver cancer cell line Huh-7. miR-328-3p overexpression significantly increased the ratio of cleaved cas3/cas3 and Bax/Bcl-2 and elevated the cell apoptosis rate of liver cancer cell line Huh-7. Simultaneously, miR-328-3p overexpression significantly increased the expression of E-cadherin in Liver cancer cell line Huh-7, accompanied by a significant decrease of N-cadherin expression. These results proved that overexpression of miR-328-3p inhibited cell proliferation, invasion, and induced apoptosis of liver cancer cell line Huh-7.

ERMP1 is a novel potential oncogene involved in oxidative stress defense and unfolded protein response (UPR), which highly expressed in various cancer (18,19). It has become a new trend that mirRNA targeted *ERMP1* to inhibit cancer development. It had reported that *ERMP1* was a good target of miR-148b, and miR-148b could suppress cell proliferation and regulated the oxidative stress response by downregulating *ERMP1* (20). In the present study, a double luciferase reporter assay showed that miR-328-3p can significantly inhibit the fluorescence intensity of *ERMP1* 3'-UTR-WT vector, but could not inhibit the fluorescence intensity of *ERMP1* 3'-UTR-MUT vector. Compared with the pcDNA-*ERMP1* transfected group,

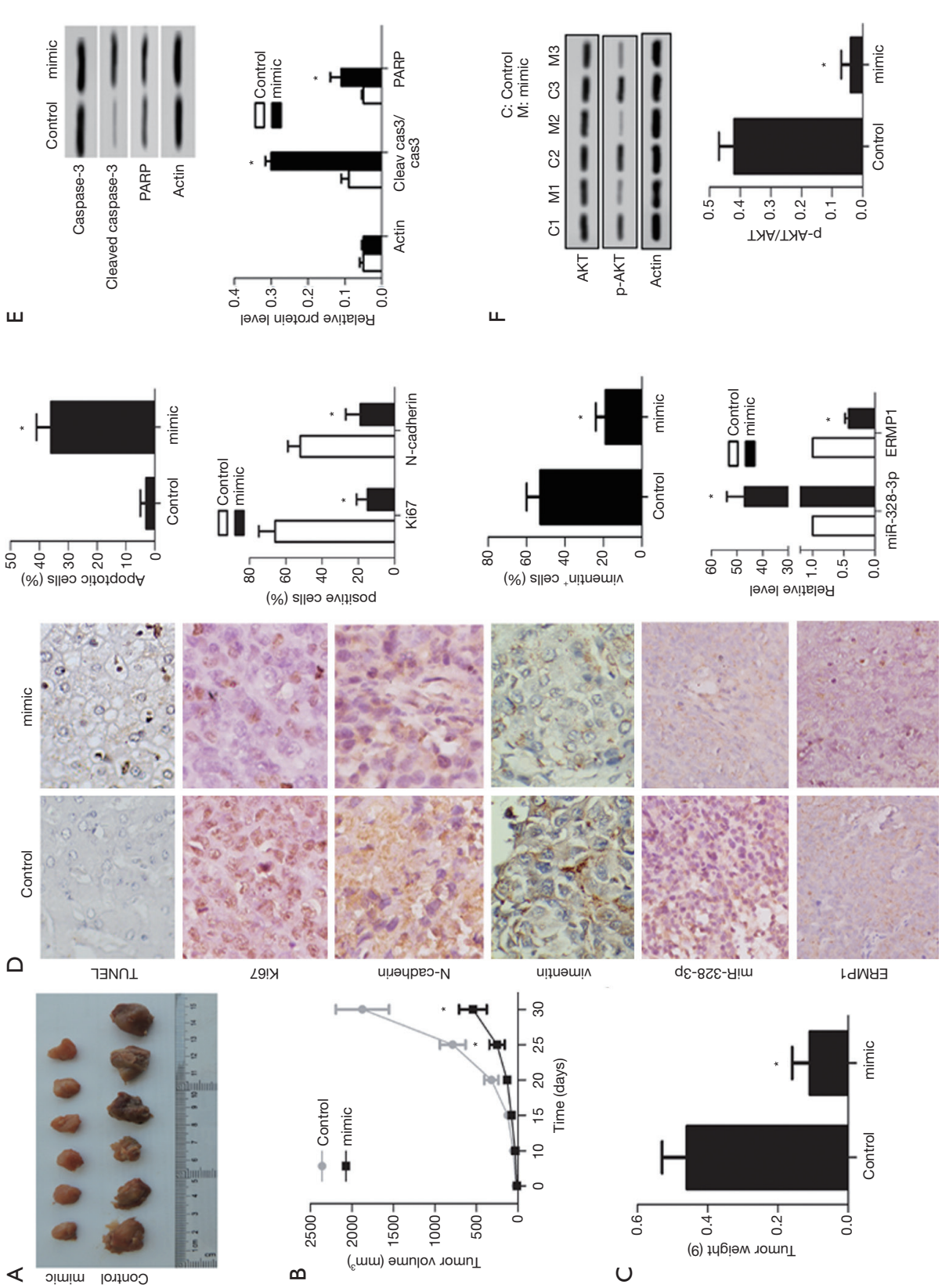

Figure 5 miR-328-3p overexpression affects tumor formation *in vivo*. (A) Tumor tissue; (B) tumor volume; (C) tumor weight; (D) immunohistochemistry typical images of Ki67, N-cadherin, vimentin, miR-328-3p and *ERMP1* (stained with SignalStain DAB Substrate Kit, ×400 magnification) and TUNEL typical images in tumor tissue (stained with FD Apop Kit, ×400 magnification); (E) Western blot typical images and relative protein level of cleav cas3/cas3 and PARP; (F) Western blot typical images and the ratio of p-AKT and AKT. Data are expressed as mean ± SD of three independent experiments. *, $P<0.05$ *vs.* control.

colony formation rate and the number of invasive cells per field were significantly decreased in the miR-328-3p mimic and pcDNA-*ERMP1* co-transfected group, while the cell apoptosis rate was significantly enhanced. These results suggest that miR-328-3p inhibits proliferation, invasion and promotes apoptosis of lung cancer cells by targeting *ERMP1*.

EMT is an indispensable part of embryonic development and organogenesis, which characterized by decreasing in epithelial and increase of mesenchymal properties. EMT is currently considered to be one of the keys and initial links in the invasion and metastasis of tumor cells (29). EMT is generally recognized as a critical factor in the dissociation of cancer cells from primary tumors and subsequent infiltration into blood vessels (30). In our study, miR-328-3p overexpression significantly mitigated the EMT of Huh-7 cells.

PI3K/AKT pathway plays a vital role in cancer stem cells (CSCs), including the ability to maintain colony-formation ability and proliferation (8). At the same time, targeting the PI3K/AKT pathway could immensely reduce the bulk tumor burden and slow down CSCs metabolism (9,10). Studies showed that the PI3K/AKT pathway engaged in the development of liver cancer. Xu *et al.* reported that growth differentiation factor 15 (GDF15) induces growth and metastasis of human liver cancer stem-like cells via AKT/GSK-3β/β-catenin signaling (31). Kim *et al.* reported that irradiated endothelial cells triggered IL-4/ERK/AKT signaling axis activity, which enhanced the malignancy of liver cancer cells (32). Xu *et al.* found that TGFβRII knockdown resulted in the suppression of cell proliferation, invasion, and induced cell apoptosis via inhibiting PI3K/Akt and p38 MAPK pathways, as well as the expression of MMPs and *ERMP1* in A549 cells (33).

In our study, compared with the pcDNA-*ERMP1* transfection group, the ratios of p-PI3K/PI3K, p-AKT/AKT, and p-mTOR/mTOR in miR-328-3p mimic and pcDNA-*ERMP1* co-transfection group were significantly decreased. These results showed that miR-328-3p inhibits phosphorylation of the PI3K/AKT pathway by targeting *ERMP1*.

Conclusions

miR-328-3p overexpression inhibits AKT phosphorylation to attenuate the malignant proliferation and invasion of liver cancer via targeting *ERMP1*. Also, *in vitro* validation experiments, smaller volume and lighter weight of transplanted tumors were observed in a miR-328-3p group compared with the control group, which consistent with the results of cell experiments. Thence, miR-328-3p might be a promising regulation of liver cancer.

Acknowledgments

Funding: None.

Footnote

Reporting Checklist: The authors have completed the ARRIVE reporting checklist. Available at http://dx.doi.org/10.21037/atm-20-3749

Data Sharing Statement: Available at http://dx.doi.org/10.21037/atm-20-3749

Conflicts of Interest: All authors have completed the ICMJE uniform disclosure form (available at http://dx.doi.org/10.21037/atm-20-3749). The authors have no conflicts of interest to declare.

Ethical Statement: The authors are accountable for all aspects of the work in ensuring that questions related to the accuracy or integrity of any part of the work are appropriately investigated and resolved. The animal experiments in present study were carried out according to the Guidelines for the Care and Use of NIH Experimental Animals and approved by Sichuan Academy of Medical Sciences & Sichuan Provincial People's Hospital.

References

1. Boland P, Wu J. Systemic therapy for hepatocellular carcinoma: beyond sorafenib. Chin Clin Oncol 2018;7:50.
2. Lai H, Zhang J, Zuo H, et al. Overexpression of miR-17 is correlated with liver metastasis in colorectal cancer.

Medicine 2020;99:e19265.
3. Yamamoto M, Sawada K, Kimura T. Therapeutic potential of microRNAs in the regulation of cancer energy metabolism. Ann Transl Med 2019;7:S292.
4. Lodish HF, Zhou B, Liu G, et al. Micromanagement of the immune system by microRNAs. Nat Rev Immunol 2008;8:120-30.
5. Zhang HF, Wang YC, Han YD. MicroRNA34a inhibits liver cancer cell growth by reprogramming glucose metabolism. Mol Med Rep 2018;17:4483-9.
6. Wang Y, Blelloch R. Cell cycle regulation by MicroRNAs in embryonic stem cells. Cancer Res 2009;69:4093-6.
7. Li X, Yuan M, Song L, et al. Silencing of microRNA-210 inhibits the progression of liver cancer and hepatitis B virus-associated liver cancer via targeting EGR3. BMC Med Genet 2020;21:48.
8. Zhou J, Wulfkuhle J, Zhang H, et al. Activation of the PTEN/mTOR/STAT3 pathway in breast cancer stem-like cells is required for viability and maintenance. Proc Natl Acad Sci U S A 2007;104:16158-63.
9. Marhold M, Tomasich E, El-Gazzar A, et al. HIF1alpha Regulates mTOR Signaling and Viability of Prostate Cancer Stem Cells. Mol Cancer Res 2015;13:556-64.
10. Kolev VN, Wright QG, Vidal CM, et al. PI3K/mTOR dual inhibitor VS-5584 preferentially targets cancer stem cells. Cancer Res 2015;75:446-55.
11. Sun X, Meng L, Qiao W, et al. Vascular endothelial growth factor A/Vascular endothelial growth factor receptor 2 axis promotes human dental pulp stem cell migration via the FAK/PI3K/Akt and p38 MAPK signalling pathways. Int Endod J 2019;52:1691-703.
12. Srivastava AK, Banerjee A. Inhibition of miR-328-3p Impairs Cancer Stem Cell Function and Prevents Metastasis in Ovarian Cancer. Cancer Res 2019;79:2314-26.
13. Liu T, Ye P, Ye Y, et al. Circular RNA hsa_circRNA_002178 silencing retards breast cancer progression via microRNA-328-3p-mediated inhibition of COL1A1. J Cell Mol Med 2020;24:2189-201.
14. Ma W, Ma CN, Zhou NN, et al. Up-regulation of miR-328-3p sensitizes non-small cell lung cancer to radiotherapy. Sci Rep 2016;6:31651.
15. Xiao B, Chen D, Zhou Q, et al. Glutamate metabotropic receptor 4 (GRM4) inhibits cell proliferation, migration and invasion in breast cancer and is regulated by miR-328-3p and miR-370-3p. BMC Cancer 2019;19:891.
16. Yan T, Ye XX. MicroRNA-328-3p inhibits the tumorigenesis of bladder cancer through targeting ITGA5 and inactivating PI3K/AKT pathway. Eur Rev Med Pharmacol Sci 2019;23:5139-48.
17. Pan S, Ren F, Li L, et al. miR-328-3p inhibits cell proliferation and metastasis in colorectal cancer by targeting Girdin and inhibiting the PI3K/Akt signaling pathway. Exp Cell Res 2020;390:111939.
18. Grandi A, Santi A, Campagnoli S, et al. ERMP1, a novel potential oncogene involved in UPR and oxidative stress defense, is highly expressed in human cancer. Oncotarget 2016;7:63596-610.
19. Zhang N, Chen Y, Shen Y, et al. Comprehensive analysis the potential biomarkers for the high-risk of childhood acute myeloid leukemia based on a competing endogenous RNA network. Blood Cells Mol Dis 2019;79:102352.
20. Qu J, Zhang L, Li L, et al. miR-148b Functions as a Tumor Suppressor by Targeting Endoplasmic Reticulum Metallo Protease 1 in Human Endometrial Cancer Cells. Oncol Res 2018;27:81-8.
21. Ye X, Lv H. MicroRNA-519d-3p inhibits cell proliferation and migration by targeting TROAP in colorectal cancer. Biomed Pharmacother 2018;105:879-86.
22. Zhang Y, Guo X, Xiong L, et al. MicroRNA-101 suppresses SOX9-dependent tumorigenicity and promotes favorable prognosis of human hepatocellular carcinoma. FEBS Lett 2012;586:4362-70.
23. McGuire A, Brown JA, Malone C, et al. Effects of age on the detection and management of breast cancer. Cancers 2015;7:908-29.
24. Garcia-Rudaz C, Luna F, Tapia V, et al. Fxna, a novel gene differentially expressed in the rat ovary at the time of folliculogenesis, is required for normal ovarian histogenesis. Development 2007;134:945-57.
25. Gao L, Mei S, Zhang S, et al. Cardio-renal Exosomes in Myocardial Infarction Serum Regulate Proangiogenic Paracrine Signaling in Adipose Mesenchymal Stem Cells. Theranostics 2020;10:1060-73.
26. Chen W, Zhang K, Dong P, et al. Noninvasive chimeric DNA profiling identifies tumor-originated HBV integrants contributing to viral antigen expression in liver cancer. Hepatol Int 2020;14:326-37.
27. Qin L, Zhong M, Adah D, et al. A novel tumour suppressor lncRNA F630028O10Rik inhibits lung cancer angiogenesis by regulating miR-223-3p. J Cell Mol Med 2020;24:3549-59.
28. Ma L, Li J. MicroRNA-519d-3p inhibits cell proliferation and cell cycle G1/S transition in glioma by targeting CCND1. Biosci Biotechnol Biochem 2020;84:297-304.
29. De Wever O, Pauwels P, De Craene B, et al. Molecular and pathological signatures of epithelial-mesenchymal

transitions at the cancer invasion front. Histochem Cell Biol 2008;130:481-94.
30. Zhu JY, Zhou F, Yu L, et al. Epithelial-mesenchymal transition of small airway epithelium in patients receiving lung tumor surgery with normal lung function and chronic obstructive pulmonary disease. Zhonghua yi xue za zhi 2019;99:2681-6.
31. Xu Q, Xu HX, Li JP, et al. Growth differentiation factor 15 induces growth and metastasis of human liver cancer stem-like cells via AKT/GSK-3beta/beta-catenin signaling. Oncotarget 2017;8:16972-87.
32. Kim SD, Baik JS, Lee JH, et al. The malignancy of liver cancer cells is increased by IL-4/ERK/AKT signaling axis activity triggered by irradiated endothelial cells. J Radiat Res 2020;61:376-87.
33. Xu CC, Wu LM, Sun W, et al. Effects of TGF-beta signaling blockade on human A549 lung adenocarcinoma cell lines. Mol Med Rep 2011;4:1007-15.

Cite this article as: Lu H, Hu J, Li J, Lu W, Deng X, Wang X. miR-328-3p overexpression attenuates the malignant proliferation and invasion of liver cancer via targeting Endoplasmic Reticulum Metallo Protease 1 to inhibit AKT phosphorylation. Ann Transl Med 2020;8(12):754. doi: 10.21037/atm-20-3749

